

Electronic Supplementary Information

Simple Anthracene Derivatives: Different Mechanoluminescence Properties

Tailored only by a Thiophene Group.

Jun Miao, Yimeng Zhang, Ming Zhang*

Table of Contents

1. Experimental Section

Instruments and methods

2. Synthesis

Scheme S1. The synthetic route of B2T, B3T, B2TM and B3TM.

3. Figures and Table

Figure S1. UV-visible absorption spectra of B2T, B3T, B2TM, B3TM in THF solutions (10^{-5} M).

Figure S2. PL spectra of B2T (a), B3T (c), B2TM (e) and B3TM (g), (concentration = 10^{-5} M) in THF/H₂O mixture with different water fraction ($\lambda_{\text{ex}}=370$ nm). PL intensities of B2T (b), B3T (d), B2TM (f) and B3TM (h) in THF/water mixtures with different water fractions.

Figure S3. (a) PL decays of B2T, B3T, B2TM, B3TM in THF solution. (concentration = 10^{-5} M) (b) PL decays of B2T and B2TM in powder states and crystal states. (c) PL decays of B3T and B3TM in powder states and crystal states.

Figure S4. The stacking models of B2T, B3T, B2TM and B3TM in crystal in different viewing directions.

Figure S5. Single molecule conformations of B2T, B3T, B2TM and B3TM in the crystals, the dihedral angles between the anthracene and the boronic ester group (θ_1), between the anthracene and the thiophene (θ_2).

Figure S6. The intermolecular interactions including C-H \cdots π (green /violet lines), C-H \cdots O (red lines) and C-H \cdots S (blue lines) of B2T-1 and B2T-2 in B2T crystal (eight molecules).

Table S1. Summarization of the C-H \cdots π intermolecular interactions of B2T-1 and B2T-2 in B2T

crystal.

Table S2. Summarization of the C-H \cdots O and C-H \cdots S interactions of B2T-1 and B2T-2 in B2T crystal.

Figure S7. The intermolecular interactions including C-H \cdots π (green /violet lines), C-H \cdots O (red lines) and C-H \cdots S (blue lines) in B3T crystal (eight molecules).

Table S3. Summarization of the C-H \cdots π intermolecular interactions in B3T crystal.

Table S4. Summarization of the C-H \cdots O and C-H \cdots S interactions in B3T crystal.

Figure S8. The intermolecular interactions including C-H \cdots π (green /violet lines), C-H \cdots O (red lines) and C-H \cdots S (blue lines) in B2TM crystal (eight molecules).

Table S5. Summarization of the C-H \cdots π intermolecular interactions in B2TM crystal.

Table S6. Summarization of the C-H \cdots O and C-H \cdots S interactions in B2TM crystal.

Figure S9. The intermolecular interactions including C-H \cdots π (green /violet lines), C-H \cdots O (red lines) and C-H \cdots S (blue lines) in B3TM crystal (eight molecules).

Table S7. Summarization of the C-H \cdots π intermolecular interactions in B3TM crystal.

Table S8. Summarization of the C-H \cdots O and C-H \cdots S interactions in B3TM crystal.

Figure S10. Molecular dipole moments of previously reported ML materials.

Figure S11. The HOMO-LUMO levels, energy gaps and dipole moments of molecular couples in B2T crystal calculated at the B3LYP/6-31g (d, p) level.

Figure S12. The HOMO-LUMO levels, energy gaps and dipole moments of molecular couples in B2T crystal calculated at the B3LYP/6-31g (d, p) level.

Figure S13. The HOMO-LUMO levels, energy gaps and dipole moments of molecular couples in B3T crystal calculated at the B3LYP/6-31g (d, p) level.

Figure S14. The HOMO-LUMO levels, energy gaps and dipole moments of coupled molecules in B2TM crystal calculated at the B3LYP/6-31g (d, p) level.

4. Structure Information

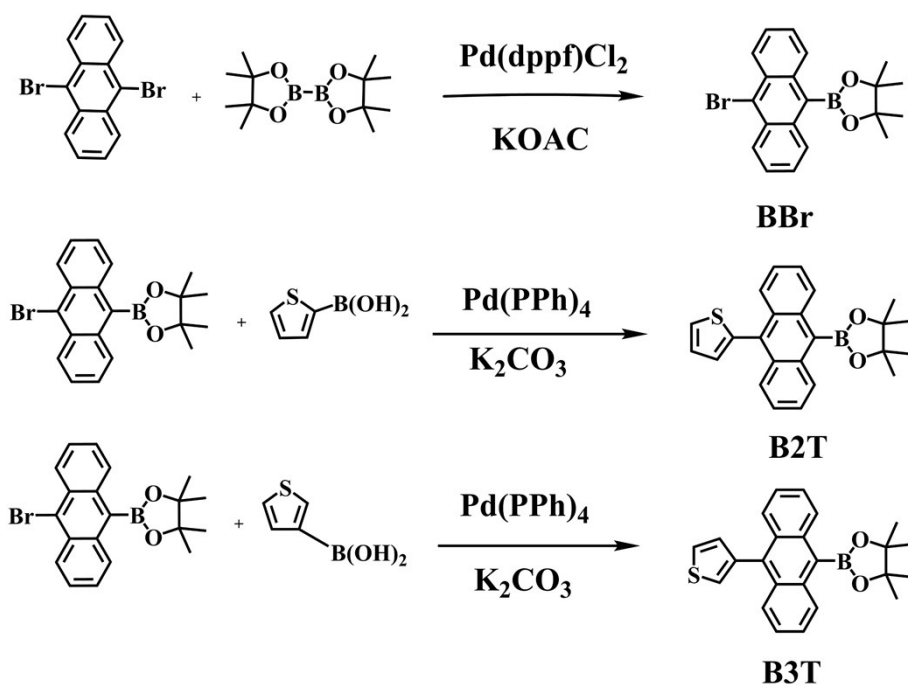
Figure S15, 16, 18, 20, 22, 23 The ^1H NMR spectrum of BABr, B2T, B3T, B2TM, BTM and B3TM.

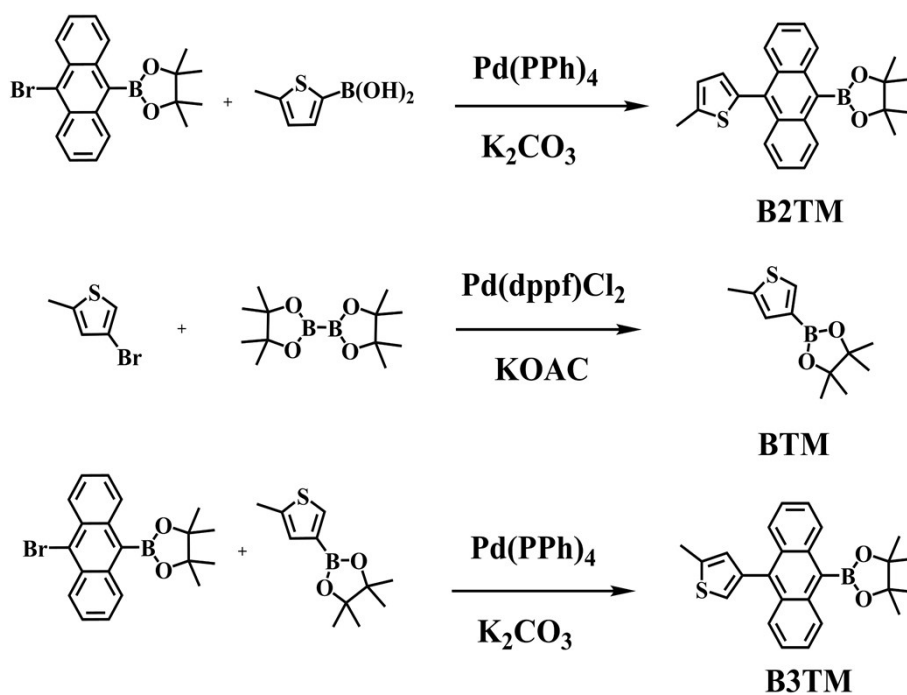
Fig. S17, 19, 21, 24 The ^{13}C NMR spectrum of B2T, B3T, B2TM and B3TM.

1. Experimental Section

Instruments and methods: ^1H and ^{13}C NMR spectra were recorded on a 500MHz Bruker AVANCZ III spectrometer, DMSO and CDCl_3 were selected as the solvent with tetramethylsilane (TMS) as the internal standard ($\delta = 0.00$ ppm). A Thermo Fisher ITQ1100 GC-MS mass detector was used to record the mass spectra. UV-vis absorption spectra was performed on UV-2550 spectrophotometer and photoluminescence spectra were recorded RF-5301PC spectrofluorophotometer. Fluorescence decay was measured on an Edinburgh FLS980 fluorescence spectrophotometer and absolute photoluminescence quantum yield (PLQY) was measured on an Edinburgh FLS920 fluorescence spectrophotometer. Thermogravimetric analysis was carried out on Q500 of thermogravimeter under nitrogen at heating rate of $10^\circ\text{C min}^{-1}$. The P-XRD (powder X-ray diffraction) patterns were recorded on a Rigaku SmartLab (3) diffractometer at a scan rate of $5^\circ/\text{min}$. The ML spectra were measured on Ocean Optics spectrometer as a power detector. The single-crystal X-ray diffraction data were recorded by a R-Axis RAPID diffractometer. The ground state (S_0) geometry was obtained from the single crystal structure and no further geometry optimization was conducted in order to maintain the specific molecular configuration and corresponding intermolecular locations.

2. Synthesis





Scheme S1. The synthetic routs of B2T, B3T, B2TM, B3TM

BBr: To a 250 mL round-bottom flask fitted with a reflux condenser, 9, 10-dibromoanthracene (2 g, 5.95 mmol), bis-(pinacolato)diboron (2.27 g, 8.93 mmol) and KOAc (1.75 g, 17.86 mmol) were dissolved in 1,4-dioxane (150 mL). Pd(dppf)Cl₂ (2.00 g, 0.30 mmol) was added and the reaction mixture was stirred at 85 °C under N₂ for 24 h. After the reaction completed, the mixture was cooled to room temperature and then water (50 mL) was added, and extracted with dichloromethane for three times (3 x 50 mL). The organic layer was dried over anhydrous Na₂SO₄. Solvent was evaporated under vacuum and the crude product was purified by column chromatography on silica gel (eluent: petroleum ether/ dichloromethane, 2/1, v/v), to obtained light green solid of BBr (1.83g, 80.2%). ¹H NMR (500 MHz, DMSO) δ 8.50 (d, J = 8.8 Hz, 2H), 8.28 (d, J = 8.6 Hz, 2H), 7.76 – 7.70 (m, 2H), 7.70 – 7.63 (m, 2H), 1.54 (s, 12H). MS (ESI), m/z: 383.85, calcd for C₂₀H₂₀BBrO₂:383.07.

B2T: To a 250 mL round-bottom flask fitted with a reflux condenser, BBr (1 g, 2.61 mmol), 2-thiopheneboronic acid (0.5 g, 3.92 mmol), K₂CO₃ (6.5 mL, 2 M) and THF (75 mL) were added. Pd(PPh₃)₄ (0.15 g, 0.13 mmol) was added and the reaction mixture was stirred at 78 °C under N₂ for 12 h. After the reaction completed, the mixture was cooled to room temperature and then water (50 mL) was added, and extracted with dichloromethane for three times (3 x 50 mL). The organic layer was dried over anhydrous Na₂SO₄. Solvent was evaporated under vacuum and the crude product

was purified by column chromatography on silica gel (eluent: petroleum ether/ dichloromethane, 2/1, v/v), to obtained light yellow solid of B2T (0.742 g, 73.6%). ¹H NMR (500 MHz, DMSO) δ 8.29 (d, *J* = 8.7 Hz, 2H), 7.92 (d, *J* = 5.2 Hz, 1H), 7.74 (d, *J* = 8.7 Hz, 2H), 7.58 (dd, *J* = 11.3, 3.9 Hz, 2H), 7.53 – 7.48 (m, 2H), 7.39 (dd, *J* = 5.1, 3.4 Hz, 1H), 7.29 – 7.25 (m, 1H), 1.55 (s, 12H). ¹³C NMR (126 MHz, CDCl₃, δ): 139.25, 135.15, 131.33, 131.24, 129.35, 128.37, 127.10, 126.62, 125.52, 125.36, 84.59, 25.24. MS (ESI), *m/z*: 385.88, calcd for C₂₄H₂₃BO₂S:386.15.

B3T: To a 250 mL round-bottom flask fitted with a reflux condenser, BBr (1 g, 2.61 mmol), 3-thiopheneboronic acid (0.5 g, 3.92 mmol), K₂CO₃ (6.5 mL, 2 M) and THF (75 mL) were added. Pd(PPh₃)₄ (0.15 g, 0.13 mmol) was added and the reaction mixture was stirred at 78 °C under N₂ for 12 h. After the reaction completed, the mixture was cooled to room temperature and then water (50 mL) was added, and extracted with dichloromethane for three times (3 x 50 mL). The organic layer was dried over anhydrous Na₂SO₄. Solvent was evaporated under vacuum and the crude product was purified by column chromatography on silica gel (eluent: petroleum ether/ dichloromethane, 2/1, v/v), to obtained white solid of B3T (0.818g, 81.3%). ¹H NMR (500 MHz, DMSO) δ 8.30 (d, *J* = 8.7 Hz, 2H), 7.89 (dd, *J* = 4.8, 2.9 Hz, 1H), 7.71 – 7.65 (m, 3H), 7.59 – 7.54 (m, 2H), 7.46 (ddd, *J* = 8.6, 6.5, 1.0 Hz, 2H), 7.24 (dd, *J* = 4.9, 1.2 Hz, 1H), 1.55 (s, 12H). ¹³C NMR (126 MHz, CDCl₃, δ): 138.83, 135.39, 134.58, 130.88, 130.34, 128.46, 127.23, 125.51, 125.40, 125.02, 84.52, 25.26. MS (ESI), *m/z*: 385.88, calcd for C₂₄H₂₃BO₂S:386.15.

B2TM: To a 250 mL round-bottom flask fitted with a reflux condenser, BBr (1 g, 2.61 mmol), 5-Methylthiophene-2-boronic acid (0.55 g, 3.91 mmol), K₂CO₃ (6.5 mL, 2 M) and THF (75 mL) were added. Pd(PPh₃)₄ (0.15 g, 0.13 mmol) was added and the reaction mixture was stirred at 78 °C under N₂ for 12 h. After the reaction completed, the mixture was cooled to room temperature and then water (50 mL) was added, and extracted with dichloromethane for three times (3 x 50 mL). The organic layer was dried over anhydrous Na₂SO₄. Solvent was evaporated under vacuum and the crude product was purified by column chromatography on silica gel (eluent: petroleum ether/ dichloromethane, 2/1, v/v), to obtained light yellow solid of B2TM (0.78g, 74.8%). ¹H NMR (500 MHz, DMSO) δ 8.28 (d, *J* = 8.6 Hz, 2H), 7.83 (d, *J* = 8.7 Hz, 2H), 7.61 – 7.56 (m, 2H), 7.53 – 7.48 (m, 2H), 7.08 – 7.02 (m, 2H), 2.62 (s, 3H), 1.55 (s, 12H). ¹³C NMR (126 MHz, CDCl₃, δ): 141.05, 136.76, 131.82, 131.32, 129.24, 128.34, 127.25, 125.49, 125.24, 84.54, 25.23, 15.42. MS (ESI), *m/z*:400.40, calcd for C₂₅H₂₅BO₂S:400.17.

BTM: To a 100 mL round-bottom flask fitted with a reflux condenser, 4-Bromo-2-methylthiophene (1 g, 5.65 mmol), bis-(pinacolato)diboron (2.15 g, 8.47 mmol) and KOAC (1.66 g, 16.9 mmol) were dissolved in 1,4-dioxane (150 mL). Pd(dppf)Cl₂ (0.21 g, 0.28 mmol) was added and the reaction mixture was stirred at 85 °C under N₂ for 24 h. After the reaction completed, the mixture was cooled to room temperature and then water (50 mL) was added, and extracted with dichloromethane for three times (3 x 50 mL). The organic layer was dried over anhydrous Na₂SO₄. Solvent was evaporated under vacuum and the crude product was purified by column chromatography on silica gel (eluent: petroleum ether/ dichloromethane, 4/1, v/v), to obtained light yellow solid of BTM (1.06 g, 84.3%). ¹H NMR (500 MHz, DMSO) δ 7.72 (d, J = 0.8 Hz, 1H), 6.95 (s, 1H), 2.45 (s, 3H), 1.26 (s, 12H). MS (ESI), m/z: 223.96, calcd for C₁₁H₁₇BO₂S:224.10.

B3TM: To a 250 mL round-bottom flask fitted with a reflux condenser, BBr (1 g, 2.61 mmol), BTM (0.88 g, 3.91 mmol), K₂CO₃ (10 mL, 2M), methylbenzene (15 mL) and ethyl alcohol (5 mL) were added. Pd(PPh₃)₄ (0.15 g, 0.13 mmol) was added and the reaction mixture was stirred at 85 °C under N₂ for 12 h. After the reaction completed, the mixture was cooled to room temperature and then water (50 mL) was added, and extracted with dichloromethane for three times (3 x 50 mL). The organic layer was dried over anhydrous Na₂SO₄. Solvent was evaporated under vacuum and the crude product was purified by column chromatography on silica gel (eluent: petroleum ether/ dichloromethane, 2/1, v/v), to obtained white solid of B3TM(0.830 g, 79.6%). ¹H NMR (500 MHz, DMSO) δ 8.29 (d, J = 8.7 Hz, 2H), 7.75 (d, J = 8.8 Hz, 2H), 7.59 – 7.52 (m, 2H), 7.49 – 7.43 (m, 2H), 7.39 (s, 1H), 6.93 (s, 1H), 2.61 (s, 3H), 1.55 (s, 12H). ¹³C NMR (126 MHz, CDCl₃, δ): 139.63, 138.61, 135.40, 135.18, 130.26, 129.17, 128.42, 127.38, 125.49, 124.92, 122.81, 84.49, 25.26, 15.42. MS (ESI), m/z:399.94, calcd for C₂₅H₂₅BO₂S:400.17.

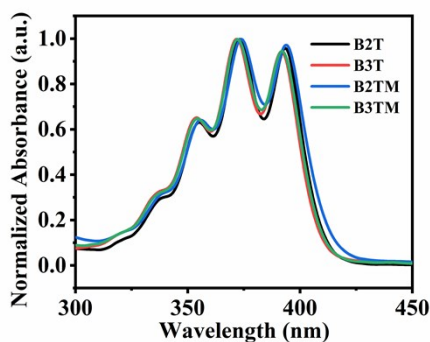


Figure S1. UV-visible absorption spectra of B2T, B3T, B2TM, B3TM in THF solutions (10⁻⁵M).

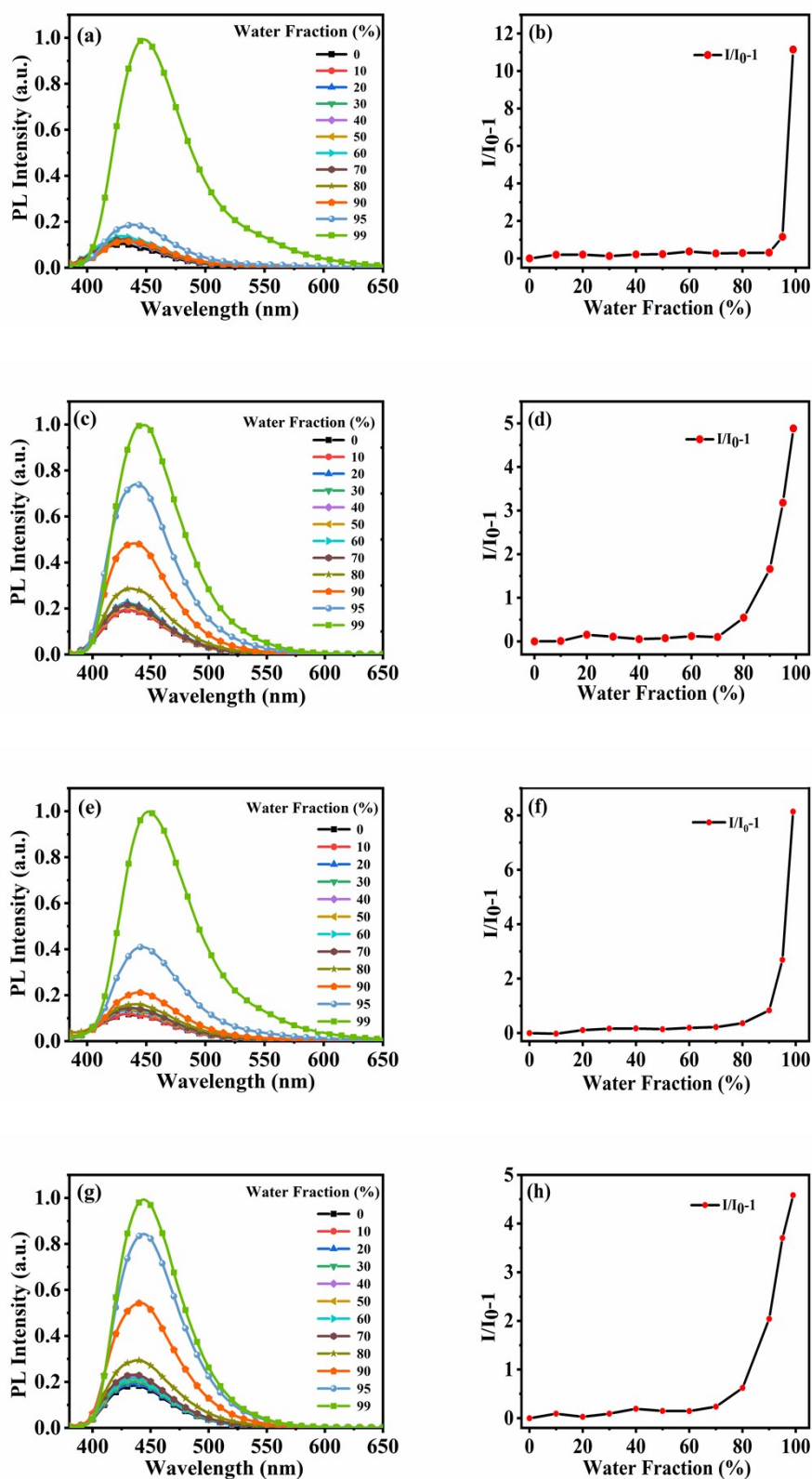


Figure S2. PL spectra of B2T (a), B3T (c), B2TM (e) and B3TM (g), (concentration =10⁻⁵ M) in THF/H₂O mixture with different water fraction. (λ_{ex} =370 nm) PL intensities of B2T (b), B3T (d), B2TM (f) and B3TM (h) in THF/water mixtures with different water fractions.

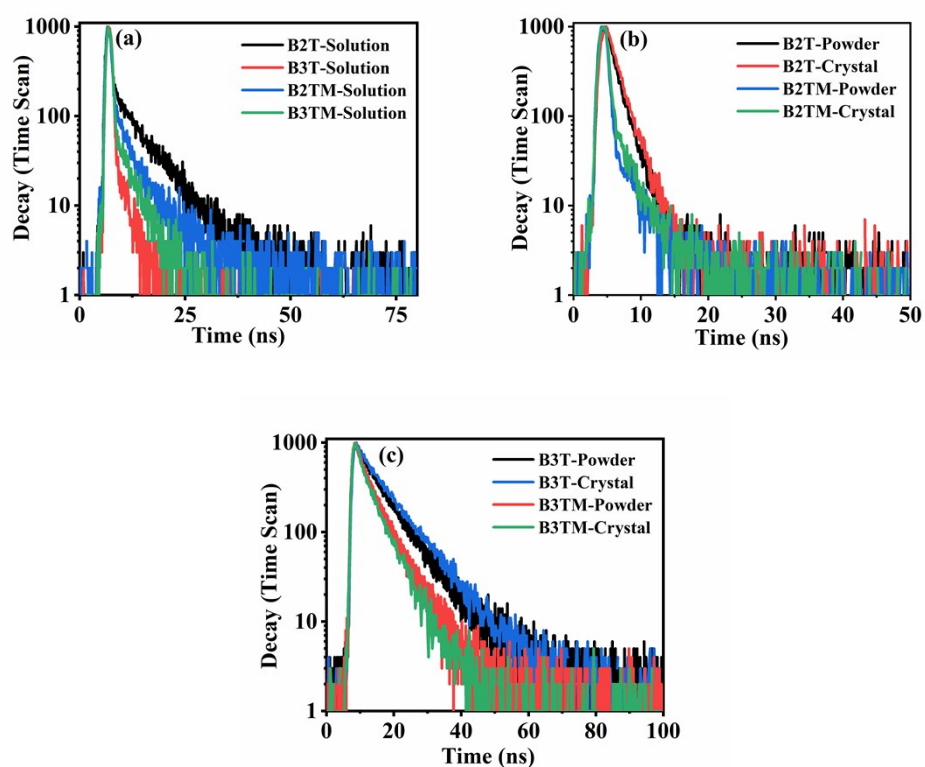
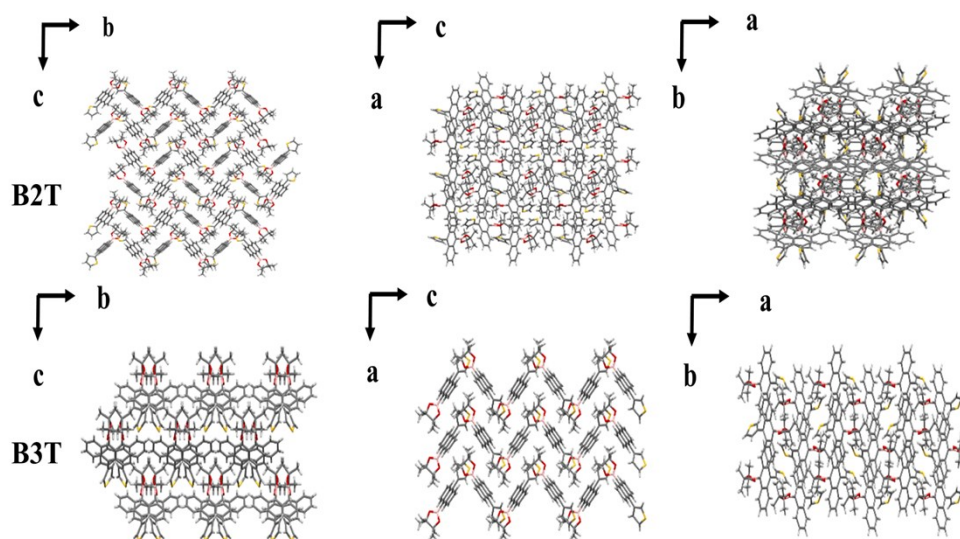


Figure S3. (a) PL decays of B2T, B3T, B2TM, B3TM in THF solution. (concentration = 10^{-5} M) (b) PL decays of B2T and B2TM in powder states and crystal states. (c) PL decays of B3T and B3TM in powder states and crystal states.



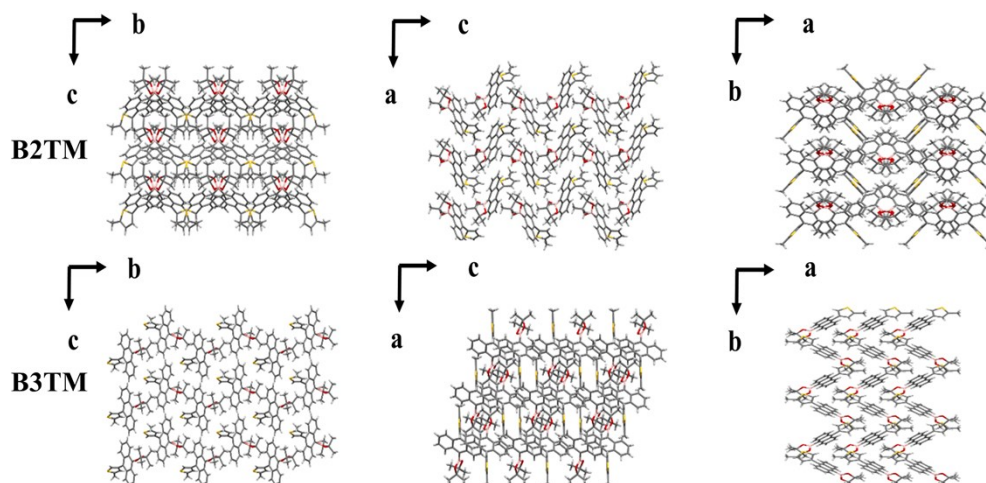


Figure S4. The stacking models of B2T, B3T, B2TM and B3TM in crystal in different viewing directions.

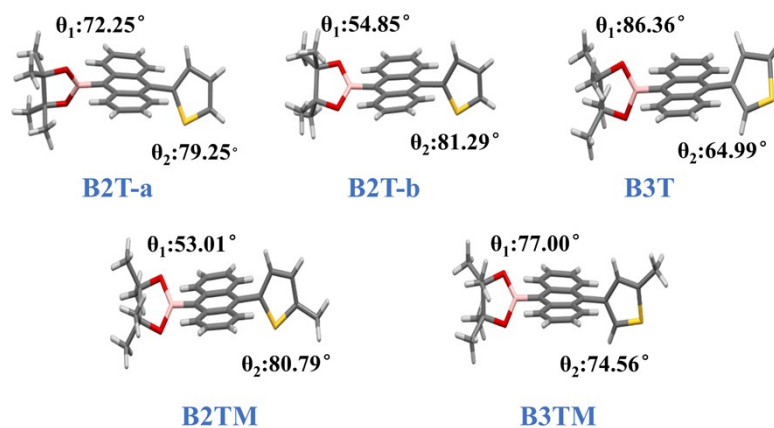


Figure S5. Single molecule conformations of B2T, B3T, B2TM and B3TM in the crystals, the dihedral angles between the anthracene and the boronic ester group (θ_1), between the anthracene and the thiophene (θ_2).

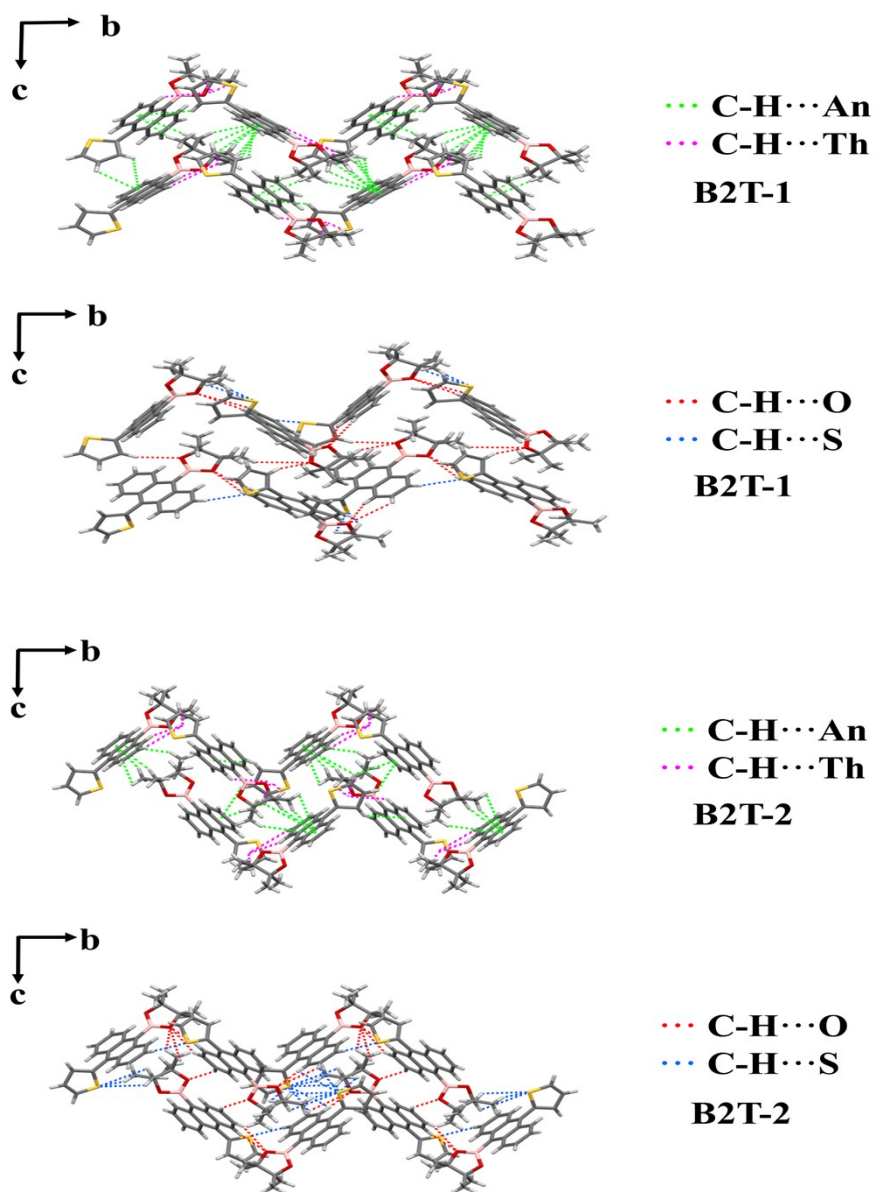


Figure S6. The intermolecular interactions including C-H⋯ π (green /violet lines), C-H⋯O (red lines) and C-H⋯S (blue lines) of B2T-1 and B2T-2 in B2T crystal (eight molecules).

Table S1. Summarization of the C-H⋯ π intermolecular interactions of B2T-1 and B2T-2 in B2TM crystal.

Molecule	Orientation of Interaction	d /Å	Number	
B2T-1	1	C-H⋯An	3.109	4
	2	C-H⋯An	3.309	4
	3	C-H⋯An	2.669	4
	4	C-H⋯An	2.946	4
	5	C-H⋯An	3.745	3
	6	C-H⋯An	3.980	3

	7	C-H...An	3.857	3
	8	C-H...An	2.986	3
	9	C-H...An	3.856	3
	10	C-H...An	3.622	3
	1	C-H...Th	3.663	3
	2	C-H...Th	3.943	3
	3	C-H...Th	3.576	3
	4	C-H...Th	3.867	3
	5	C-H...Th	3.385	3
	6	C-H...Th	3.327	3
B2T-2	1	C-H...An	3.949	4
	2	C-H...An	2.912	4
	3	C-H...An	2.906	4
	4	C-H...An	3.993	4
	5	C-H...An	3.745	2
	6	C-H...An	2.282	2
	7	C-H...An	3.368	2
	8	C-H...An	3.506	2
	1	C-H...Th	3.663	4
	2	C-H...Th	3.943	4
	3	C-H...Th	3.576	4
	4	C-H...Th	3.867	2
	5	C-H...Th	3.385	2
	6	C-H...Th	3.327	2

Table S2. Summarization of the C-H...O and C-H...S interactions of B2T-1 and B2T-2 in B2TM crystal

Molecule		Orientation of Interaction	d /Å	Number
B2T-1	1	C-H...O	2.662	4
	2	C-H...O	2.963	3
	3	C-H...O	3.035	3
	4	C-H...O	3.550	3
	5	C-H...O	3.453	3
	6	C-H...O	3.429	3
	1	C-H...S	3.562	3
	2	C-H...S	3.966	3
	3	C-H...S	2.949	3
B2T-2	1	C-H...O	2.963	4
	2	C-H...O	3.035	4
	3	C-H...O	3.580	4
	4	C-H...O	3.872	2
	5	C-H...O	3.913	2

Molecule	Orientation of Interaction	d /Å	Number
6	C-H···O	3.550	2
7	C-H···O	3.453	2
1	C-H···S	3.422	4
2	C-H···S	3.316	4
3	C-H···S	3.845	4
4	C-H···S	2.949	4
5	C-H···S	3.966	2
6	C-H···S	3.562	2
7	C-H···S	3.421	2
8	C-H···S	3.429	2

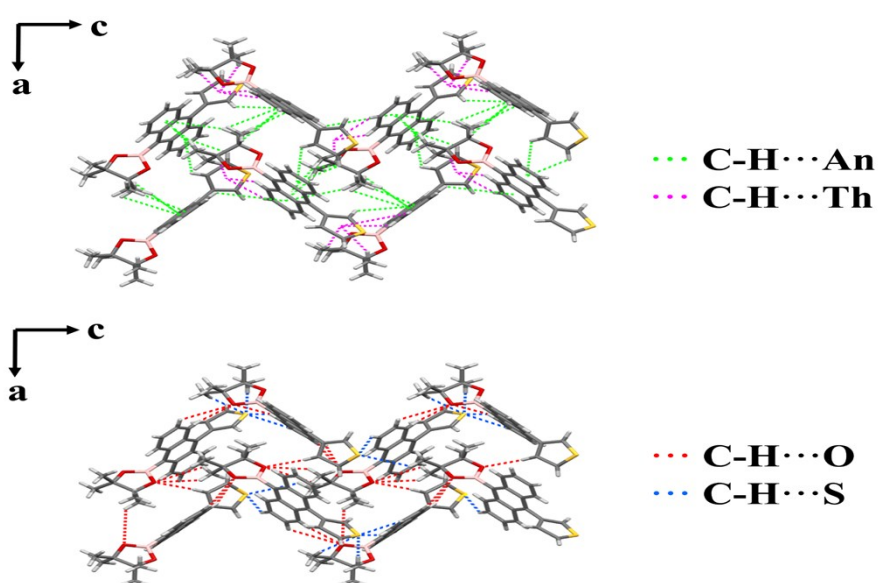


Figure S7. The intermolecular interactions including C-H··· π (green /violet lines), C-H···O (red lines) and C-H···S (blue lines) in B3T crystal (eight molecules).

Table S3. Summarization of the C-H··· π intermolecular interactions in B3T crystal.

Molecule	Orientation of Interaction	d /Å	Number	
B3T	1	C-H···An	2.893	4
	2	C-H···An	2.577	4
	3	C-H···An	3.922	4
	4	C-H···An	3.624	4
	5	C-H···An	3.788	4
	6	C-H···An	3.034	4
	7	C-H···An	3.294	3
	8	C-H···An	3.276	3
	9	C-H···An	3.347	3
	10	C-H···An	3.989	3
	11	C-H···An	3.820	3

1	C-H...Th	3.570	3
2	C-H...Th	3.746	3
3	C-H...Th	3.264	3
4	C-H...Th	3.987	3
5	C-H...Th	3.920	3
6	C-H...Th	3.875	3
7	C-H...Th	3.674	3

Table S4. Summarization of the C-H...O and C-H...S interactions in B3T crystal.

Molecule	Orientation of Interaction	d /Å	Number	
B3T	1	C-H...O	3.921	4
	2	C-H...O	2.645	4
	3	C-H...O	3.179	3
	4	C-H...O	3.340	3
	5	C-H...O	3.458	3
	6	C-H...O	3.309	3
	7	C-H...O	3.212	3
	8	C-H...O	3.850	3
	1	C-H...S	3.334	3
	2	C-H...S	3.536	3
	3	C-H...S	3.047	3
	4	C-H...S	2.964	3
	5	C-H...S	2.997	3
6	C-H...S	3.623	3	

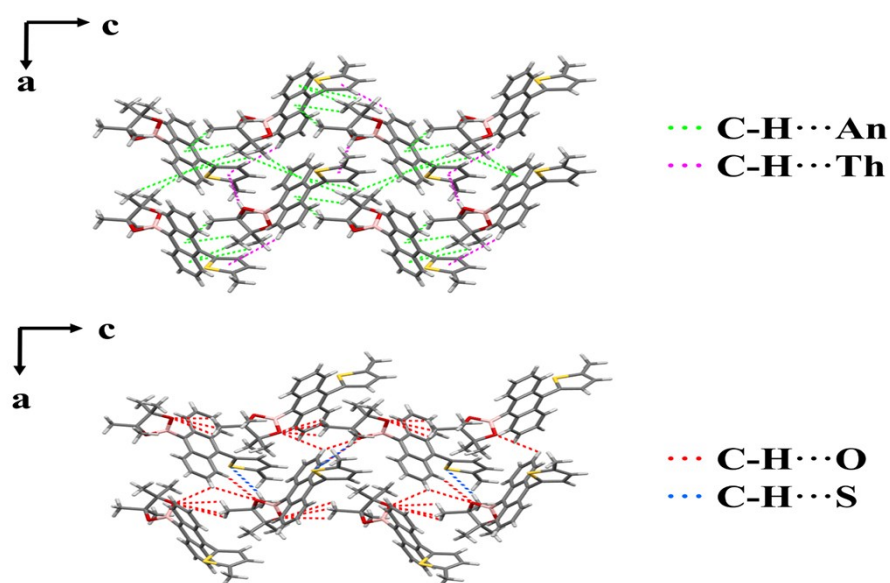


Figure S8. The intermolecular interactions including C-H... π (green /violet lines), C-H...O (red lines) and C-H...S (blue lines) in B2TM crystal (eight molecules).

Table S5. Summarization of the C-H $\cdots\pi$ intermolecular interactions in B2TM crystal.

Molecule	Orientation of Interaction	d /Å	Number	
B2TM	1	C-H \cdots An	3.374	6
	2	C-H \cdots An	2.860	6
	3	C-H \cdots An	3.170	6
	4	C-H \cdots An	3.876	6
	5	C-H \cdots An	3.180	4
	6	C-H \cdots An	3.372	4
	1	C-H \cdots Th	3.844	5
	2	C-H \cdots Th	2.986	3

Table S6. Summarization of the C-H \cdots O and C-H \cdots S interactions in B2TM crystal

Molecule	Orientation of Interaction	d /Å	Number	
B2TM	1	C-H \cdots O	3.572	6
	2	C-H \cdots O	2.960	6
	3	C-H \cdots O	2.997	6
	4	C-H \cdots O	3.260	4
	5	C-H \cdots O	3.110	3
	6	C-H \cdots O	3.076	3
	1	C-H \cdots S	3.500	3

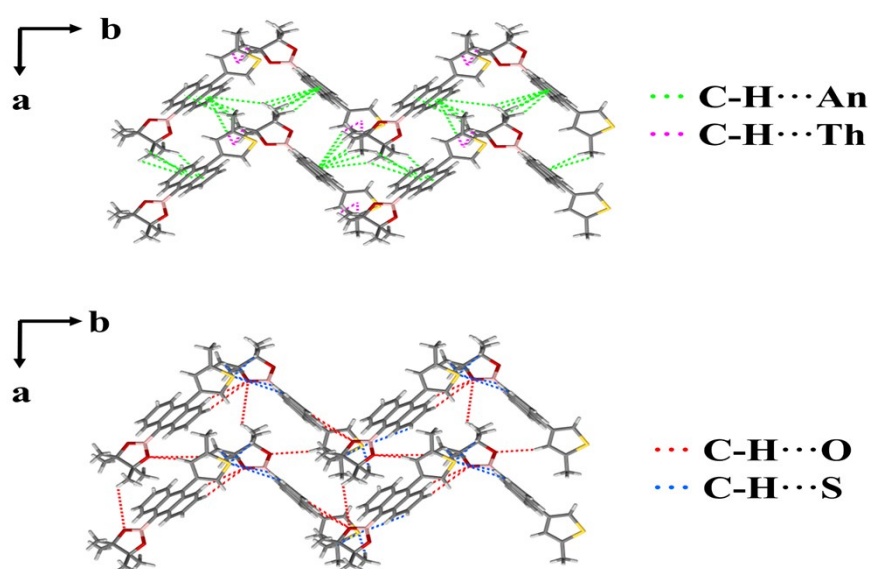


Figure S9. The intermolecular interactions including C-H $\cdots\pi$ (green /violet lines), C-H \cdots O (red lines) and C-H \cdots S (blue lines) in B3TM crystal (eight molecules).

Table S7. Summarization of the C-H $\cdots\pi$ intermolecular interactions in B3TM crystal.

Molecule	Orientation of Interaction	d /Å	Number	
B3TM	1	C-H \cdots An	3.617	4
	2	C-H \cdots An	2.945	4
	3	C-H \cdots An	3.855	4
	4	C-H \cdots An	3.017	4
	5	C-H \cdots An	3.947	4
	6	C-H \cdots An	2.635	4
	7	C-H \cdots An	3.940	4
	8	C-H \cdots An	3.829	3
	9	C-H \cdots An	2.822	3
	10	C-H \cdots An	3.597	3
	11	C-H \cdots An	3.675	3
	1	C-H \cdots Th	3.043	6
	2	C-H \cdots Th	3.725	6

Table S8. Summarization of the C-H \cdots O and C-H \cdots S interactions in B3TM crystal.

Molecule	Orientation of Interaction	d /Å	Number	
B3TM	1	C-H \cdots O	3.071	6
	2	C-H \cdots O	3.725	6
	3	C-H \cdots O	3.839	6
	4	C-H \cdots O	2.989	4
	5	C-H \cdots O	3.880	2
	1	C-H \cdots S	3.345	6
	2	C-H \cdots S	3.517	6
	3	C-H \cdots S	3.164	6
	4	C-H \cdots S	3.722	6

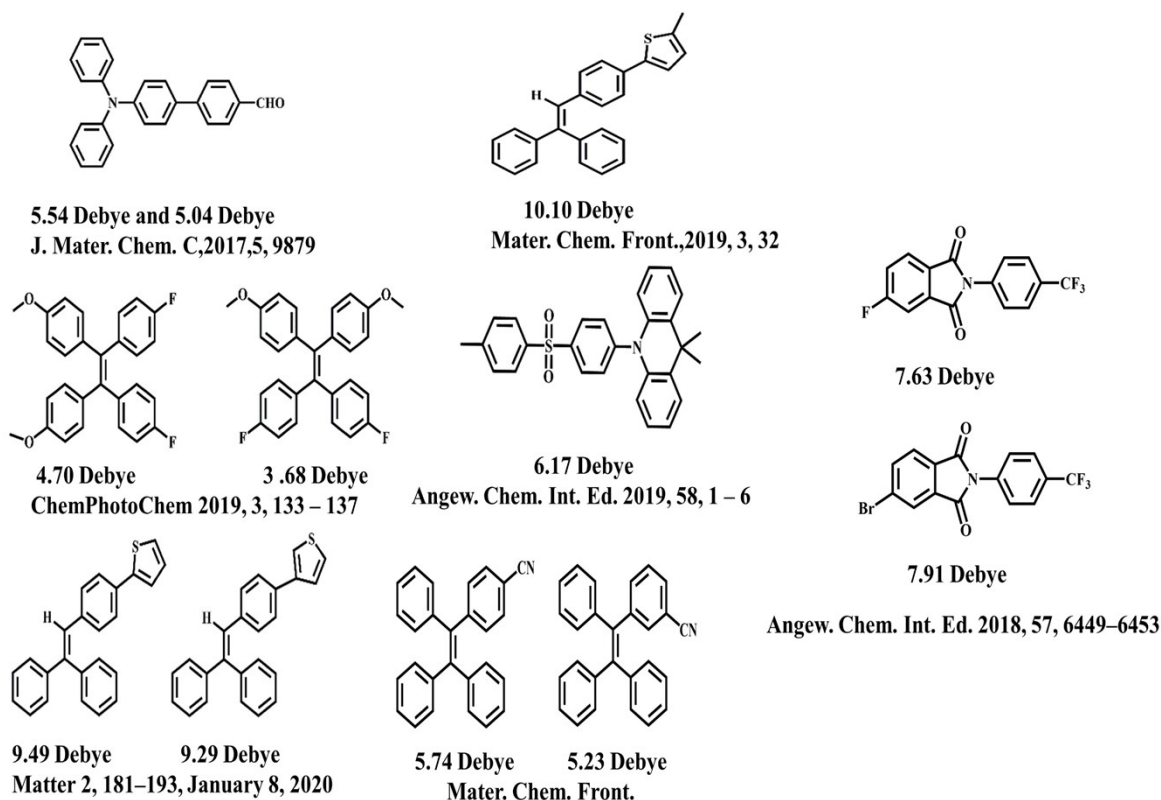


Figure S10. Molecular dipole moments of previously reported ML materials.

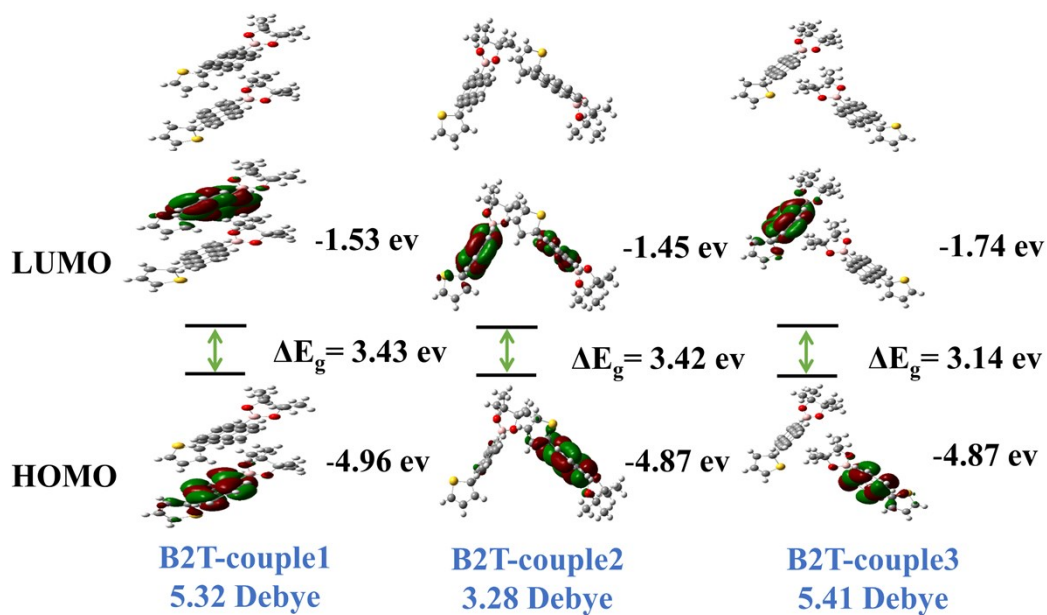


Figure S11. The HOMO-LUMO levels, energy gaps and dipole moments of coupled molecules in B2T crystal calculated at the B3LYP/6-31g (d, p) level.

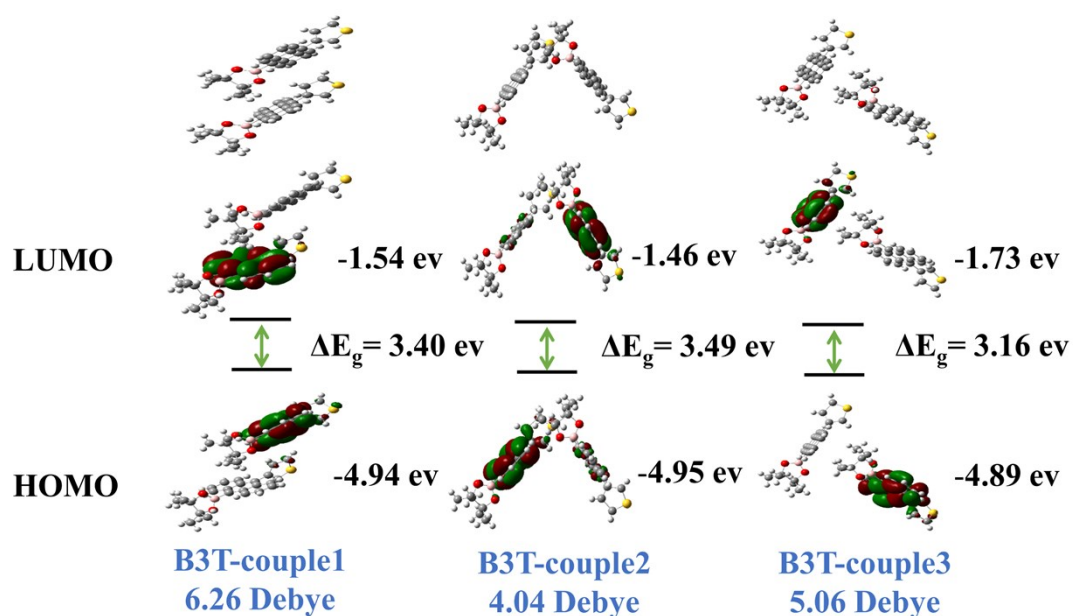


Figure S12. The HOMO-LUMO levels, energy gaps and dipole moments of coupled molecules in B3T crystal calculated at the B3LYP/6-31g (d, p) level.

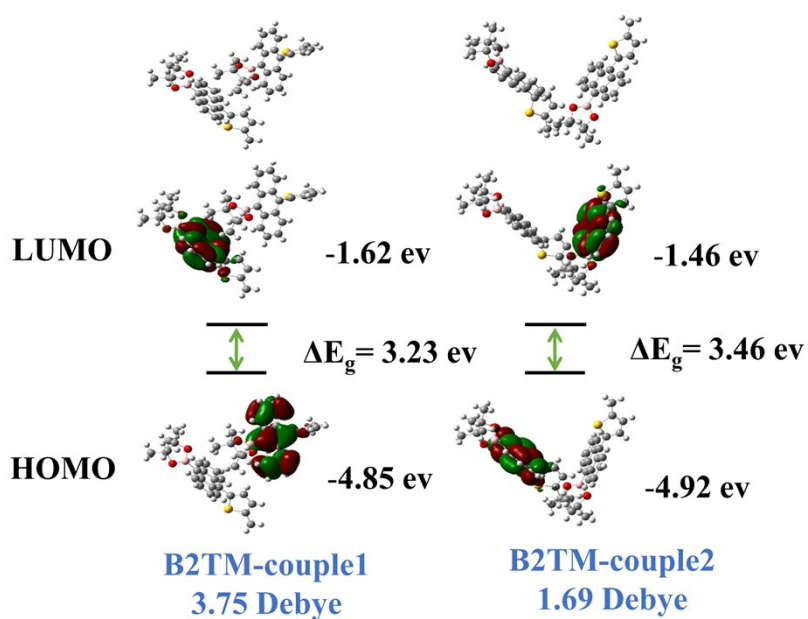


Figure S13. The HOMO-LUMO levels, energy gaps and dipole moments of coupled molecules in B2TM crystal calculated at the B3LYP/6-31g (d, p) level.

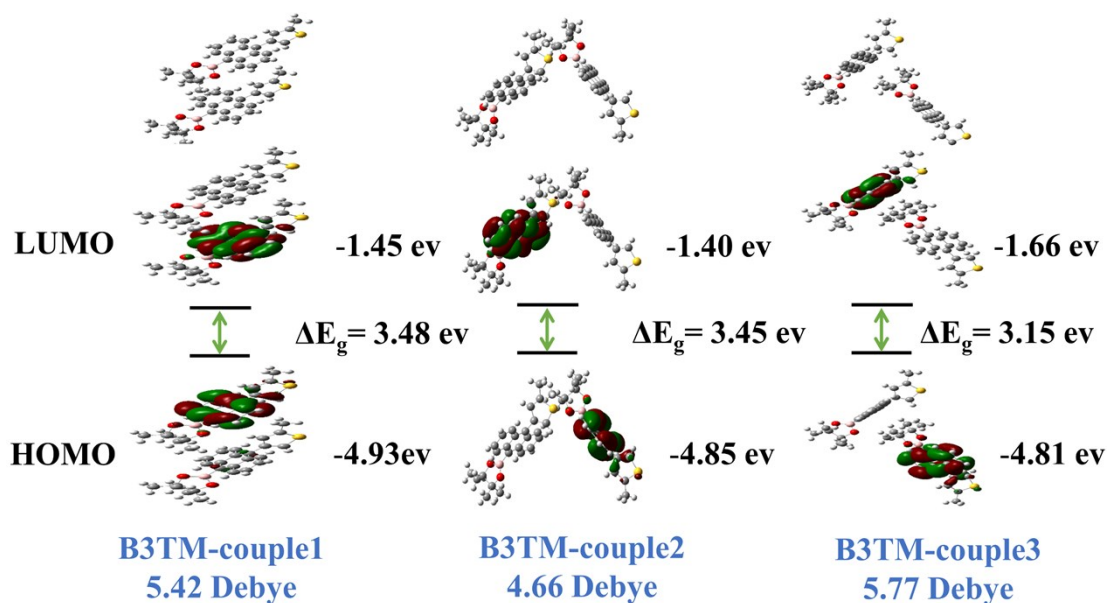


Figure S14. The HOMO-LUMO levels, energy gaps and dipole moments of coupled molecules in B2TM crystal calculated at the B3LYP/6-31g (d, p) level.

Table S9. Structural data crystal of B2T, B3T, B2TM and B3TM.

Name	B2T	B3T	B2TM	B3TM
Empirical formula	C ₂₄ H ₂₃ BO ₂ S	C ₂₄ H ₂₃ BO ₂ S	C ₂₅ H ₂₅ BO ₂ S	C ₂₅ H ₂₅ BO ₂ S
Wavelength (Å)	0.71073	0.71073	0.71073	0.71073
Crystal system	monoclinic	orthorhombic	orthorhombic	monoclinic
Space group	P2 ₁ /c	Pna2 ₁	Pca2 ₁	P2 ₁
Unit cell Angles (°)	$\alpha=90$	$\alpha=90$	$\alpha=90$	$\alpha=90$
	$\beta=91.514(4)$	$\beta=90$	$\beta=90$	$\beta=110.932(5)$
	$\gamma=90$	$\gamma=90$	$\gamma=90$	$\gamma=90$
Unit cell lengths (Å)	a=10.8058(13)	a=14.8406(6)	a=16.8951(7)	a=7.7785(12)
	b=13.2428(14)	b=10.9093(5)	b=9.8379(4)	b=14.866(2)
	c=28.753(3)	c=12.4824(6)	c=13.0652(5)	c=10.1560(17)
Unit cell volume (Å ³)	4113.0(8)	2020.91(16)	2171.60(15)	1096.9(3)
Z	8	4	4	2
Density (g/cm ³)	1.248	1.270	1.224	1.212
F (000)	1632.0	816.0	848.0	424.0
CCDC number	2048017	2048018	2048019	2048020

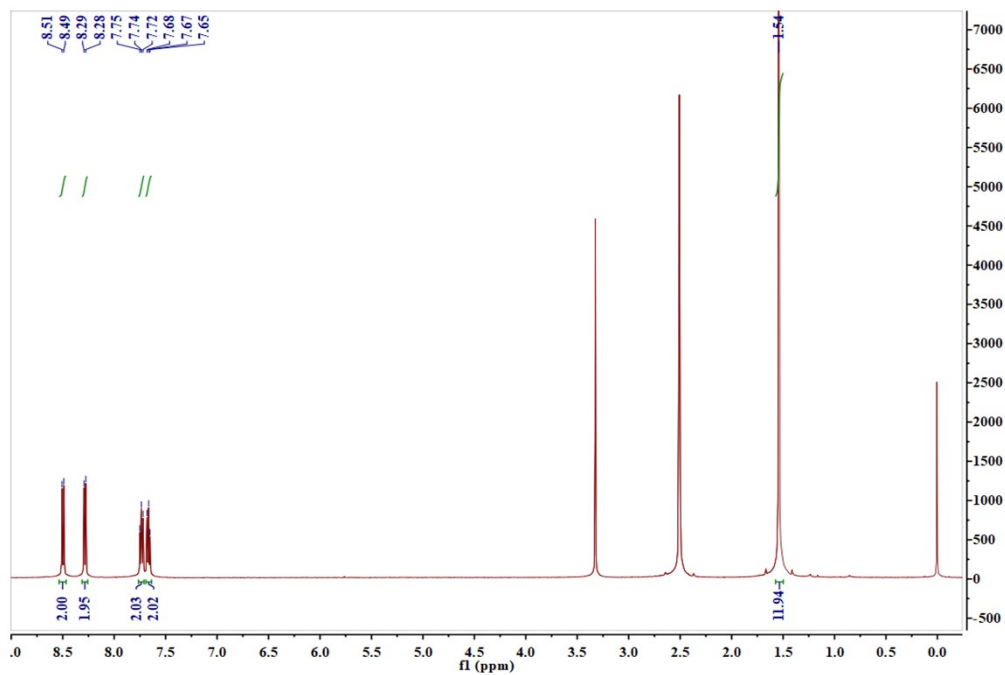


Figure S15. The ^1H NMR spectrum of BABr.

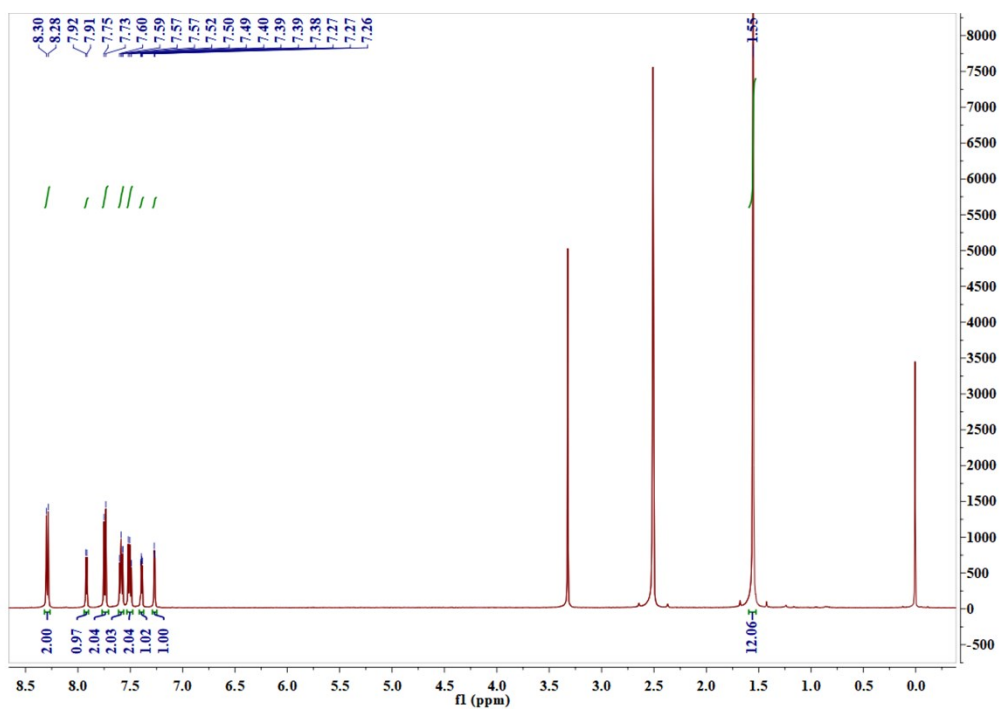


Figure S16. The ^1H NMR spectrum of B2T.

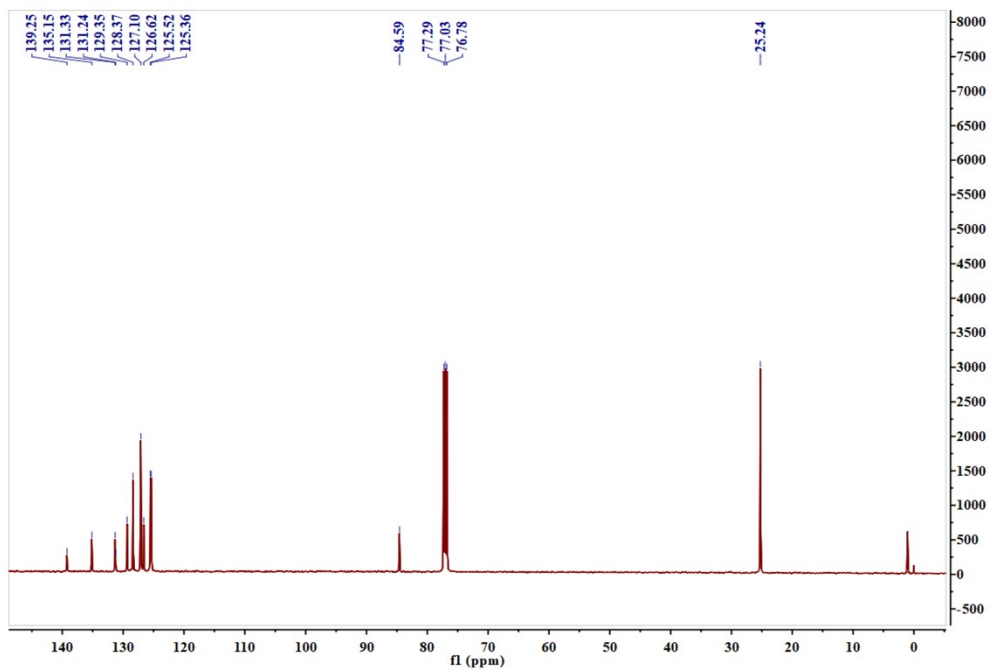


Figure S17. The ^{13}C NMR spectrum of B2T.

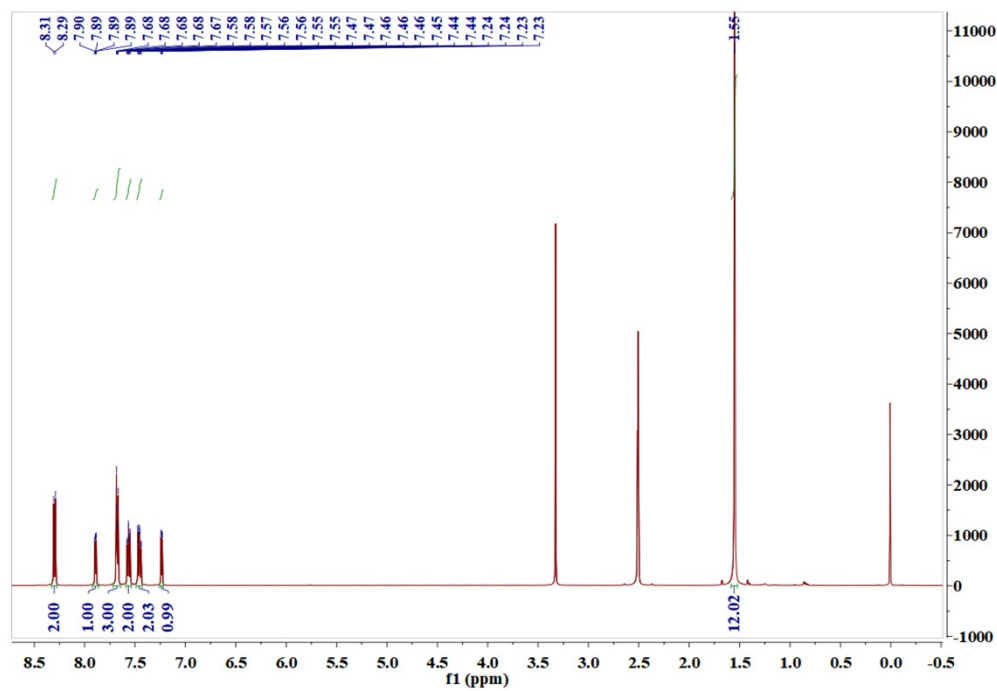


Figure S18. The ^1H NMR spectrum of B3T.

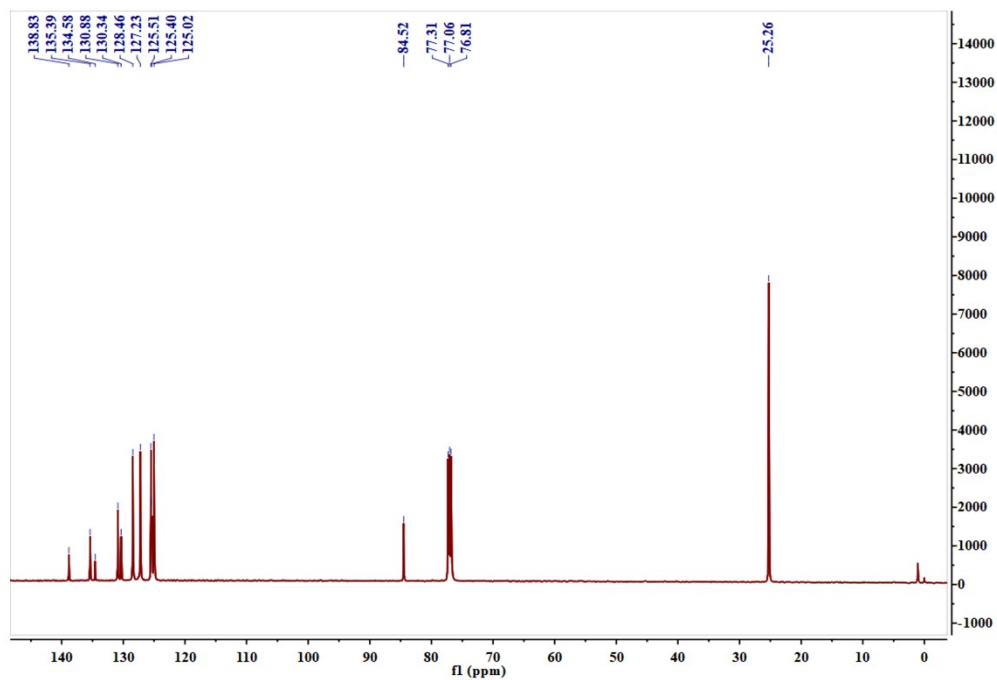


Figure S19. The ^{13}C NMR spectrum of B3T.

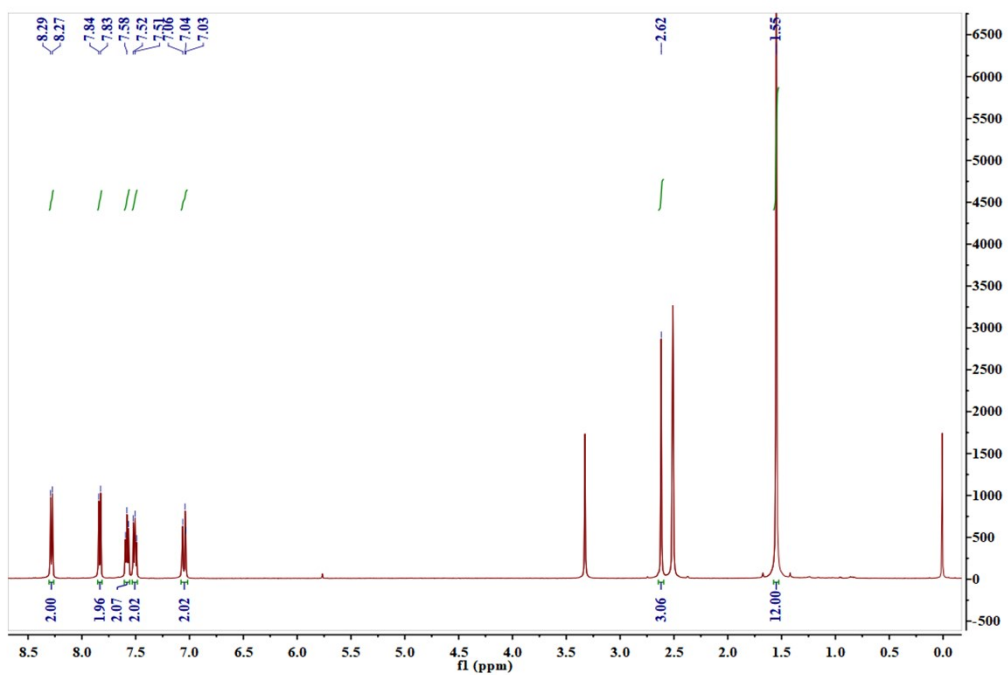


Figure S20. The ^1H NMR spectrum of B2TM.

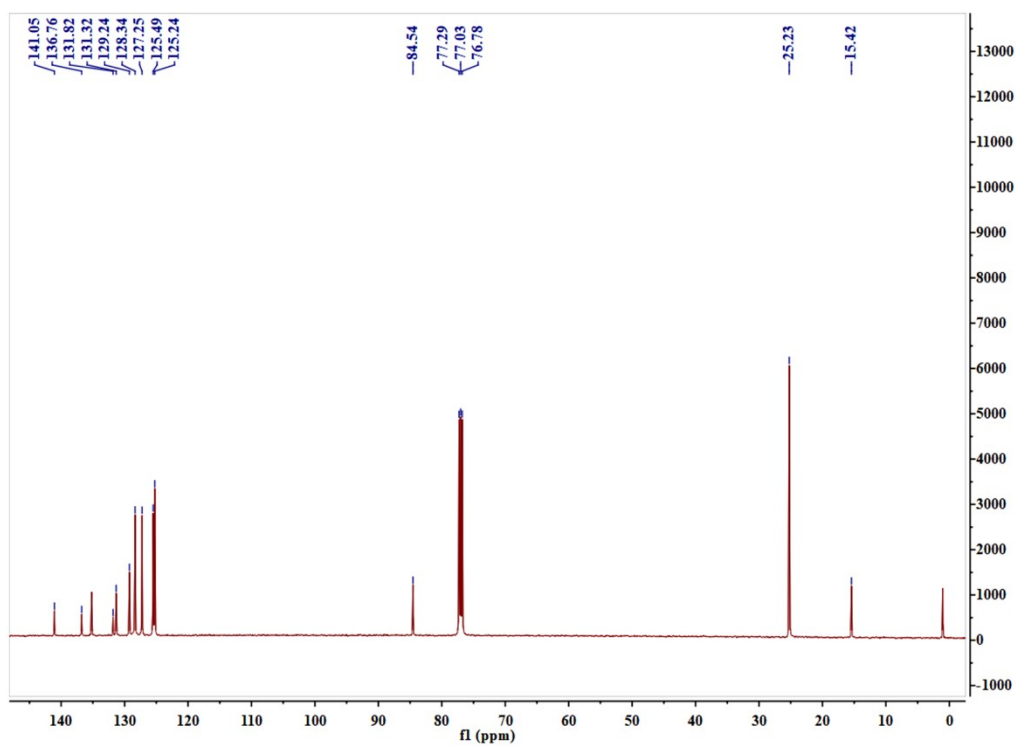


Figure S21. The ^{13}C NMR spectrum of B2TM.

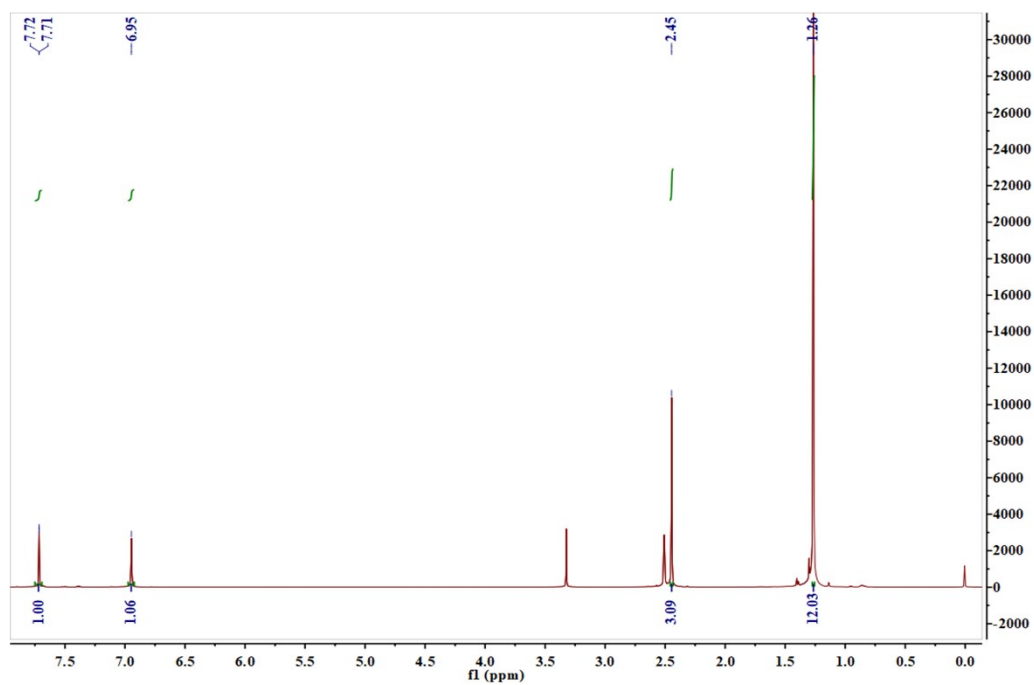


Figure S22. The ^1H NMR spectrum of BTM.

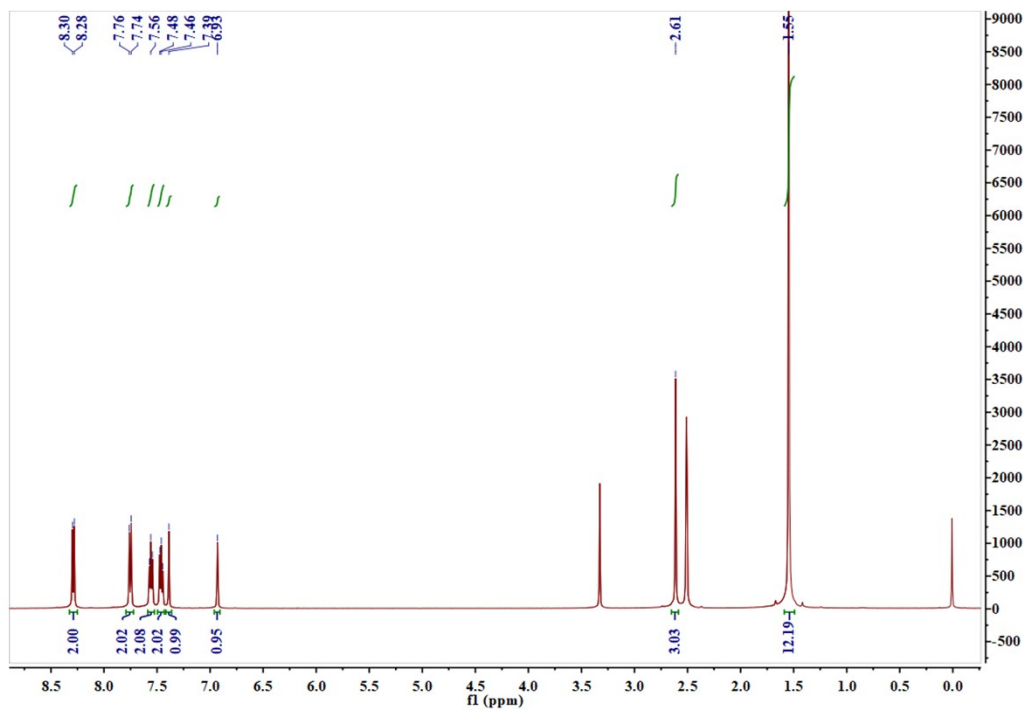


Figure S23. The ^1H NMR spectrum of B3TM.

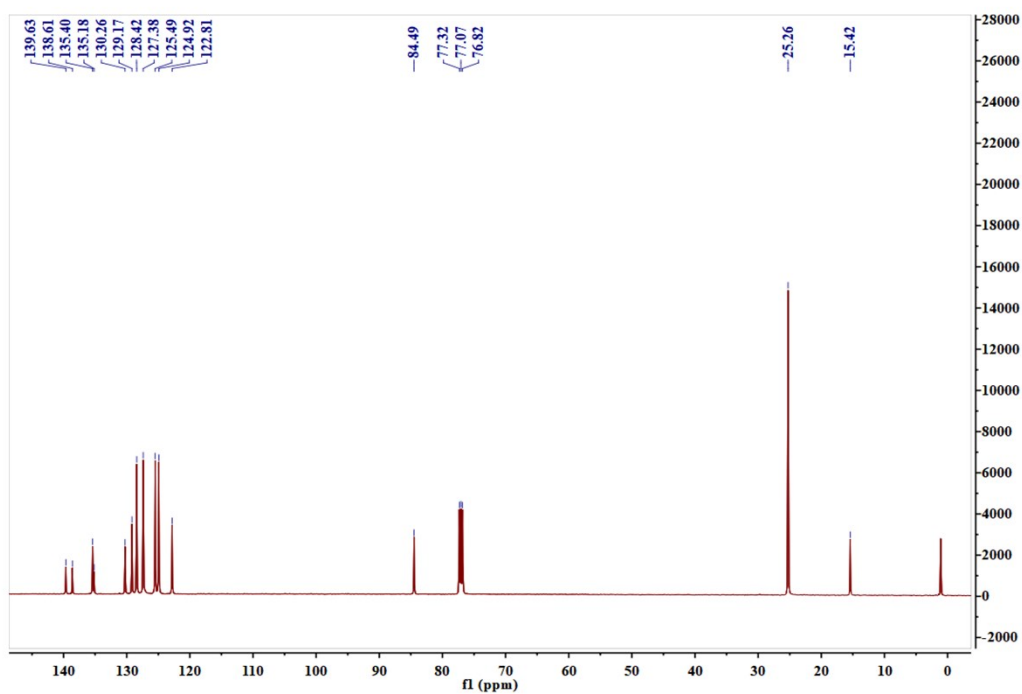


Figure S24. The ^{13}C NMR spectrum of B3TM.